

論文 / 著書情報
Article / Book Information

Title	Determination of surface polarity of c-axis oriented ZnO films by coaxial impact-collision ion scattering spectroscopy
Authors	T. Ohnishi,A. Ohtomo,M. Kawasaki,K. Takahashi,H. Koinuma
Citation	Applied Physics Letters, Vol. 72, No. 7,
Pub. date	1998, 2
URL	http://scitation.aip.org/content/aip/journal/apl
Copyright	Copyright (c) 1998 American Institute of Physics

Determination of surface polarity of *c*-axis oriented ZnO films by coaxial impact-collision ion scattering spectroscopy

T. Ohnishi,^{a),b)} A. Ohtomo,^{c)} M. Kawasaki,^{c)} K. Takahashi,^{b),d)} M. Yoshimoto,^{b)}
and H. Koinuma^{b),e)}

Tokyo Institute of Technology, 4259 Nagatsuta, Midori-ku Yokohama 226, Japan

(Received 10 September 1997; accepted for publication 15 December 1997)

We have identified the surface polar structure of wurtzite-type ZnO films by coaxial impact-collision ion scattering spectroscopy. High-quality ZnO epitaxial films were prepared on sapphire (α -Al₂O₃) (0001) substrates by laser molecular beam epitaxy using a ZnO ceramic target. The (000 $\bar{1}$) crystallographic plane (the O face) was found to terminate the top surface of the ZnO film by comparing spectra of the films with those of well-defined (0001) and (000 $\bar{1}$) surfaces of bulk single crystals. The preferential [000 $\bar{1}$] growth direction of ZnO films is discussed from the viewpoints of the chemical interaction at the interface and surface stability against sublimation.

© 1998 American Institute of Physics. [S0003-6951(98)02907-6]

Among metaloxides, ZnO has been extensively studied because it can be used in many versatile applications such as transparent conductive films, sensors, transducers, surface acoustic wave devices, and as a catalyst. Recently, we found that excitonic ultraviolet (390 nm) laser emission occurs when high-quality ZnO films are optically pumped by a frequency-tripled Nd:YAG (355 nm) laser beam.¹ These films were deposited on sapphire (0001) substrates by laser molecular beam epitaxy (laser MBE) resulting in *c*-axis oriented heteroepitaxy. The films were composed of hexagonally shaped nanocrystals, which had coalesced into a honeycomb-like structure. The optical properties of the films were very sensitive to the crystal quality and the size of nanocrystals. To control these factors, it is crucially important to understand the heteroepitaxy mechanism involved in such a large lattice-mismatch system.

The crystal structure of ZnO is wurtzite and the stacking sequence of atomic layers along the *c* axis is not symmetric. A crystal with its *c* axis normal to the surface, as determined by x-ray diffraction, can be either [0001] or [000 $\bar{1}$] oriented, depending on whether the (0001) Zn face or the (000 $\bar{1}$) O face forms the terminating layer. These two crystallographic planes are known to exhibit different physical² and chemical³ properties. However, the significance of the terminating atomic layer has hardly been discussed for heteroepitaxial ZnO thin films. Most of the work on this topic has been carried out by diffraction techniques such as low-energy electron diffraction (LEED)⁴ and photoelectron diffraction⁵ on single-crystal surfaces. In this work, we use coaxial impact-collision ion scattering spectroscopy (CAICISS) to investigate the surface polarity of ZnO thin films.

Low-energy ion scattering is very sensitive to the composition and structure of topmost atomic layers because of the large scattering cross section of low-energy ions.^{6,7} The

scattering angle of an ion beam impinging on a sample surface is very close to 180° in CAICISS experiments. This is achieved by the coaxial positioning of both the incident ion beam and detector for time-of-flight (TOF) analysis. In this configuration, the TOF spectrum is composed of peaks corresponding to a head-on collision between incident He ions and target atoms on the topmost surface.⁸ Hence, the surface atomic species and arrangement can be determined precisely from the incident and azimuthal angular dependences of the TOF spectrum, by taking into account the shadowing and focusing effects as was reported for SrTiO₃ in case of our previous papers.⁹

In this study, we used CAICISS to determine the surface polarity of the *c*-axis oriented ZnO films. The well-defined (0001) and (000 $\bar{1}$) surfaces of bulk ZnO single crystals were also analyzed by CAICISS for comparison.

High-quality *c*-axis oriented ZnO films were grown on sapphire (α -Al₂O₃) (0001) substrates at a temperature of 550 °C by ablating a ceramic ZnO target (99.999%) with KrF excimer laser pulses (1 J/cm²) in 1 × 10⁻⁶ Torr of O₂ gas. Commercial ZnO (0001) single crystals grown by the hydrothermal technique (Litton Airtron Co.) were used as reference samples. The single crystals were annealed at 1000 °C in air for 2 h to obtain clean and atomically well-defined surfaces. The surface morphology of the specimens was observed with an atomic force microscope [(AFM) Seiko SPI-3700].

The specimens were introduced into an ultrahigh vacuum chamber equipped with a CAICISS (Shimadzu CAICISS-I) analyzer and a two-axis computer-controlled goniometer. The CAICISS measurements were carried out at room temperature at a background pressure of less than 2 × 10⁻⁹ Torr. The He⁺ ion beam (2 keV) was chopped into pulses of 150 ns duration at a 100 kHz repetition rate. The specimen was set on the goniometer and the ion beam was focused into a 3 mm diam spot on the sample surface. The time-averaged current of the incident ion beam was about 150 pA. The backscattered ions and neutrals were detected by microchannel plates at a distance of 530 mm from the specimen to obtain the TOF spectra. During the interaction

^{a)}Electronic mail: ohnishi1@oxide.rlem.titech.ac.jp

^{b)}Materials and Structure Laboratory.

^{c)}Department of Innovative and Engineering Materials.

^{d)}On leave from Shinkosha Co. LTD.

^{e)}Also a member of CREST, Japan Science & Technology Corporation.
Electronic mail: koinuma@oxide.rlem.titech.ac.jp

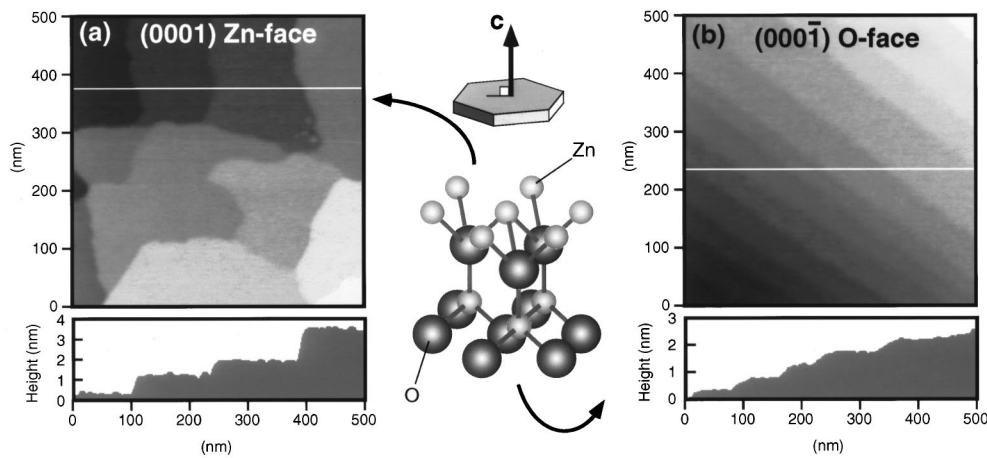


FIG. 1. AFM images (500 nm×500 nm) of ZnO single crystals annealed at 1000 °C in air: (a) (0001) surface, and (b) (000 $\bar{1}$) surface.

between incident He ions and surface atoms, part of the ions are neutralized by charge transfer. In our experimental setup, we did not intend to separate the signal of ions from that of neutral particles as in Ref. 10. If one really needs to perform detailed analysis of atomic species and position at the top-most surface, one should concentrate on the signal from ions. However, we wished to distinguish the (0001) from the (000 $\bar{1}$) surfaces of ZnO single crystals and thin films in this letter. For this purpose, we chose the advantage of high signal intensity counting from the detection of both charged and neutral species.

AFM images taken on the (0001) and (000 $\bar{1}$) surfaces (backside of each other) of an annealed single crystal are shown in Figs. 1(a) and 1(b), respectively. Atomically flat terraces and steps can be seen in both images. The step height on the (000 $\bar{1}$) surface was found to be 0.52 nm, which corresponds to a single unit cell of ZnO. The step height in the (0001) image was, typically, 2 nm, indicating that step bunching occurred during annealing. The surface morphology of a high-crystallinity ZnO thin film (200 nm thickness) is shown in the AFM image of Fig. 2. Hexagonal faceting of 0.52 nm steps is clearly visible. The typical terrace width is 20 nm, which is smaller than what we observed on the

single-crystal surface. It is still possible to carry out reasonable CAICISS measurements because the terraces are atomically flat.

Figure 3(a) shows the TOF spectrum of the ZnO (0001) single-crystal surface at normal incidence. The peak at 4600 ns corresponds to the head-on collision between the He ion and Zn atom. At normal incidence, the Zn atoms in the second layer below the surface are shadowed by the O atoms in the first layer, therefore, they do not contribute to the scattering signal. The peak at 4600 ns can thus be assigned to the He particles (ions plus neutrals), which collided with Zn atoms located in the topmost atomic layer. The tail observed for a longer TOF results from multiple scattering and/or inelastic interaction with the surface. The signal for He particles scattered by the O atoms should appear at 5540 ns but cannot be observed. This can be explained by the much smaller scattering cross section of O compared to that of Zn. As a consequence, only the Zn signal intensity dependence on both incident and azimuthal angles is discussed in this letter.

The Zn signal intensity is plotted in Fig. 4 as a function of the incident angle when the crystal was rotated in the [11 $\bar{2}$ 0] direction. As can be clearly seen in Figs. 4(a) and 4(b), the (0001) and (000 $\bar{1}$) surfaces gave quite different angular dependences. The spectrum of a thin-film sample [Fig. 4(c)] coincides with Fig. 4(b). We can, therefore, conclude

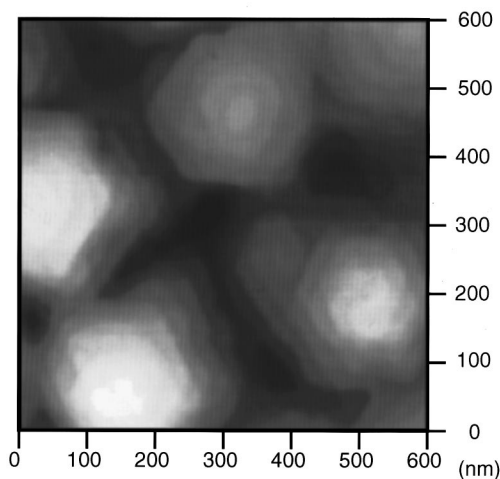


FIG. 2. An AFM image (600 nm×600 nm) of a 200 nm thick ZnO film on sapphire (0001). The step height of 0.52 nm corresponds to a single unit cell of ZnO.

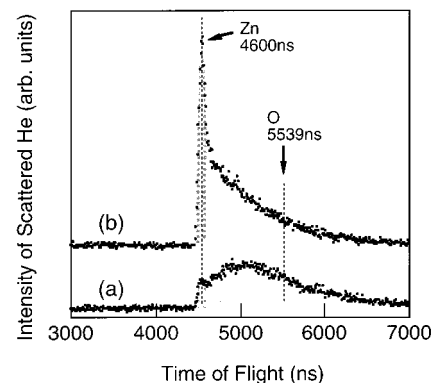


FIG. 3. Time of flight spectra of the (0001) surface of a ZnO single crystal. The incident angle was (a) normal to the surface and (b) 68°.

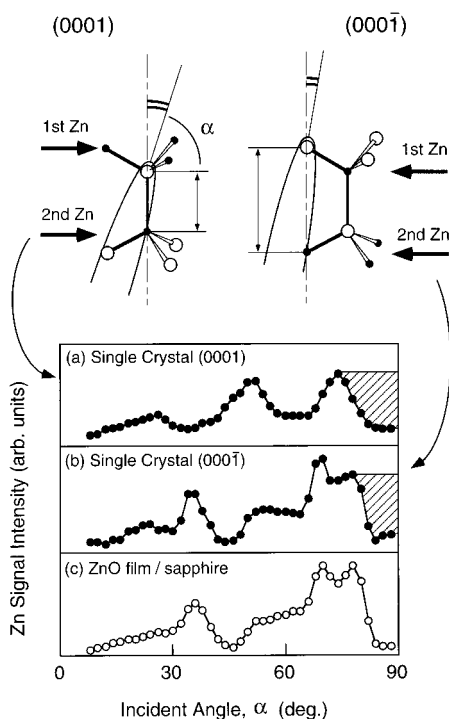


FIG. 4. Incident angular dependences of the Zn signal intensity along the $[11\bar{2}0]$ azimuth. (a) single crystal (0001), (b) single crystal (000 $\bar{1}$), and (c) thin film. The variation of the film is similar to that of the (000 $\bar{1}$) surface.

that the film surface is terminated by oxygen, i.e., the (000 $\bar{1}$) face. We also measured the signal intensity dependences on the azimuthal angle with keeping the incident angle constant. The signal variation differs very much between (0001) and (000 $\bar{1}$) surfaces of ZnO single crystal and that for the film coincided with (000 $\bar{1}$) data.

The intensity dependence of the incident angle can be analyzed by taking the shadowing and focusing effects into account. The trajectory of He ions is schematically shown in the inset of Fig. 4. As was described already, Zn atoms in the second layer are inside the shadow cones of the O atoms of the topmost layer when the incident angle is 90°. As the surface is tilted, Zn atoms in the second layer will appear at the edge of the oxygen shadow cones and focused He ions hit the second layer Zn atoms (focusing effect). At this angle, the signal intensity increases as shown in Fig. 3(b). Since the distance between the topmost O atoms and Zn atoms in the second layer is longer for the (000 $\bar{1}$) surface than for the (0001) surface, focusing should take place at a smaller tilt angle for the (000 $\bar{1}$) surface. The hatched region in Figs. 4(a) and 4(b) is considered to be the missing part of the signal from the second Zn atom due to the shadowing effect. As expected, the signal increased at a smaller tilting angle (larger α) for the (000 $\bar{1}$) surface. The entire angular dependence can be explained by considering focusing and shadowing effects. The simulation based on a three-dimensional two-atom model,¹¹ taking also surface reconstruction into account, is in progress.

We now discuss why the film has chosen the [000 $\bar{1}$] growth direction on a (0001) sapphire substrate. Recently, there have been several reports on the surface polarity of the c -axis oriented GaN films grown on sapphire (0001) substrates.^{12,13} The lattice constants of wurtzite GaN are a

$=0.319$ nm and $c=0.519$ nm, which are close to those of ZnO ($a=0.324$ nm, $c=0.520$ nm). Ion channeling analysis has revealed that GaN films grown by metalorganic chemical vapor deposition have Ga polarity, that is actually the (0001) Ga-face surface.¹² Romano *et al.* attributed the [0001] growth direction to the strong N–Al interaction at the interface of GaN and Al₂O₃.¹³ Al-terminated sapphire forced the Ga–N–Al sequence to expose the Ga layer at the film surface. Contrary to GaN, ZnO films grown on sapphire have O polarity, as found in the present work. The difference in growth atmosphere should also be taken into account: GaN is grown in a reducing (NH₃ and H₂) environment whereas ZnO is grown in an oxidizing environment. If we assume O termination for the Al₂O₃ surface because of the oxidizing atmosphere during growth, a similar reasoning can be held to explain the O polarity for ZnO as in Ref. 13.

Reevaporation of ZnO from the growing surface can also help to maintain the O polarity. Kohl *et al.* observed sublimation of ZnO from the (0001) Zn face of a single crystal by mass spectroscopy in ultrahigh vacuum at a temperature as low as 380 °C.² In contrast, sublimation was not detected from the (000 $\bar{1}$) O face even at 600 °C.² Since our film was deposited at 550 °C, selective sublimation of the (0001) Zn face domains will take place, leaving the more stable (000 $\bar{1}$) O face on the film surface.

In conclusion, we have identified the growth direction of ZnO films to be [000 $\bar{1}$] by means of CAICISS analysis of well-defined surfaces of ZnO single crystals and thin films deposited by laser MBE.

Two of the authors (T.O. and A.O.) are supported by JSPS Research Fellowships for Young Scientists. This work was supported in part by the ASPRONC Foundation, the TORAY Foundation of Japan, the RFTF program of JSPS (96P00205), and the Japan Small Business Corp., NEDO.

¹Z. K. Tang, P. Yu, G. K. L. Wong, M. Kawasaki, A. Ohtomo, H. Koinuma, and Y. Segawa, *Solid State Commun.* **103**, 459 (1996); Y. Segawa, A. Ohtomo, M. Kawasaki, H. Koinuma, Z. K. Tang, P. Yu, and G. K. L. Wong, *Phys. Status Solidi* **202**, 669 (1997).

²D. Kohl, M. Henzler, and G. Heiland, *Surf. Sci.* **41**, 403 (1974).

³A. N. Mariano and R. E. Hanneman, *J. Appl. Phys.* **34**, 384 (1963).

⁴V. E. Henrich, H. J. Zeiger, E. I. Solomon, and R. R. Gay, *Surf. Sci.* **74**, 682 (1978).

⁵M. Galeotti, A. Atrei, U. Bardi, G. Rovida, M. Torrini, E. Zanazzi, A. Santucci, and A. Klimov, *Chem. Phys. Lett.* **222**, 349 (1994).

⁶T. Buck, in *Methods of Surface Analysis*, edited by A. W. Czanderna (Elsevier, Amsterdam, 1975), p. 75.

⁷J.-M. Beuken and P. Bertrand, *Surf. Sci.* **162**, 329 (1985).

⁸M. Katayama, E. Nomura, N. Kanekama, H. Soejima, and M. Aono, *Nucl. Instrum. Methods Phys. Res. B* **33**, 857 (1988).

⁹M. Kawasaki, K. Takahashi, T. Maeda, R. Tsuchiya, M. Shinohara, O. Ishiyama, T. Yonezawa, M. Yoshimoto, and H. Koinuma, *Science* **266**, 1540 (1994).

¹⁰I. Kamiya, M. Katayama, E. Nomura, and M. Aono, *Surf. Sci.* **242**, 404 (1991).

¹¹M. Shinohara, O. Ishiyama, T. Nishihara, F. Ohtani, M. Yoshimoto, T. Maeda, and H. Koinuma, *Proceedings of the 2nd NIRIM International Symposium on Advanced Materials, Ibaraki, Japan* (National Institute for Research in Inorganic Materials, Japan, 1995), p. 203.

¹²B. Daudin, J. L. Rouviere, and M. Arlery, *Appl. Phys. Lett.* **69**, 2480 (1996).

¹³L. T. Romano, J. E. Northrup, and M. A. O'Keefe, *Appl. Phys. Lett.* **69**, 2394 (1996).